International Journal of Chemical, Materials and Biomolecular Sciences
ISSN: 2415-6620
Vol:13, No:6, 2019

Synthesis and *in vitro* Characterization of a Gel-Derived SiO_2-CaO-P_2O_5-SrO-Li_2O Bioactive Glass

Mehrnaz Aminitabar, Moghan Amirhosseinian, Morteza Elsa

***Abstract*—**Bioactive glasses (BGs) are a group of surface-reactive biomaterials used in clinical applications as implants or filler materials in the human body to repair and replace diseased or damaged bone. Sol-gel technique was employed to prepare a SiO_2-CaO-P_2O_5 glass with nominal composition of 58S BG with the addition of Sr and Li modifiers which imparts special properties to the BG. The effect of simultaneous addition of Sr and Li on bioactivity and biocompatibility, proliferation, alkaline phosphatase (ALP) activity of osteoblast cell line MC3T3-E1 and antibacterial property against methicillin-resistant *Staphylococcus aureus* (MRSA) bacteria were examined. BGs were characterized by X-ray diffraction, Fourier transform infrared spectroscopy, scanning electron microscopy before and after soaking the samples in the simulated body fluid (SBF) for different time intervals to characterize the formation of hydroxyapatite (HA) formed on the surface of BGs. Structural characterization indicated that the simultaneous presence of 5% Sr and 5% Li in 58S-BG composition not only did not retard HA formation because of opposite effect of Sr and Li of the dissolution of BG in the SBF but also, stimulated the differentiation and proliferation of MC3T3-E1s. Moreover, the presence of Sr and Li on dissolution of the ions resulted in an increase in the mean number of DAPI-labeled nuclei which was in good agreement with live/dead assay. The result of antibacterial tests revealed that Sr and Li-substituted 58S BG exhibited a potential antibacterial effect against MRSA bacteria. Because of optimal proliferation and ALP activity of MC3T3-E1cells, proper bioactivity and high antibacterial potential against MRSA, BG-5/5 is suggested as a multifunctional candidate for bone tissue engineering.

***Keywords*—**Antibacterial activity, bioactive glass, sol-gel, strontium.

I. Introduction

BGs, a subset of amorphous silicate compositions, are the first synthetic agents used in bio tissue engineering to repair and regenerate bone through their bioactivity and biocompatibility [1]. Previous studies have documented that BGs have the capability to form stable chemical bonds to both hard and soft tissues by the function of the bone-like hydroxycarbonate apatite (HCA) layer on their surfaces upon contact with SBF [2]. When BGs are planted in the body and in contact with body fluids or in SBF, a high surface area polycrystalline HCA is formed by the mechanisms that previously suggested by Hench and Wilson [3].

In bone tissue engineering applications, the composition of the BGs are modified by adding different elements such as strontium [4], magnesium [5], zinc [6], copper [7], silver [8] or lithium [9] in order to enhance their bioactivity and biocompatibility. When in contact with SBF, the dissolution of ions from the BGs has been recognized to stimulate the human body's response to certain properties, for instance, osteoconduction [10] and antibacterial activity properties [11]. The biological response of human cells to ionic dissolution products was recently reviewed by Hoppe et al. [12].

In recent years, much research has been done in clinical bone tissue engineering to investigate the individual effects of Sr and Li in the body. For example, it was reported that the substitution of Sr for Ca in BG composition led to a reduced bone resorption and accelerated bone remodeling processes because of the reduction of osteoclast activity and the improvement of the replication of preosteoblast cells [13]. Therefore, Sr^{2+}/Ca^{2+} has been substituted in BGs to improve their bioactivity [14].

Lithium has been applied for bone fracture healing and orthopedic implants [15]. Many studies have been done to investigate the influence of Li on bone density in the body [16]. Han et al. showed that Li intensifies the proliferation and differentiation in human periodontal ligament-derived cells [17] and increases osteogenic differentiation in mesenchymal stem cells (MSCs) [17]. Additionally, treatment with lithium enhances bone formation and improves bone mass [18]. Khorami et al. reported the proliferation rate of osteoblastic cells and alkaline phosphate activity in Li-substituted glasses were improved compared to Li-free samples [19]. Moreover, Li has antidepressant and immune-stimulating properties as well as antimicrobial properties [20]. Also, biodegradability and bioactivity are improved in lithium-modified bioglasses (Li-BGs) [21]. Bioactivity is affected not only by composition [22] but also by synthesis methods: the sol-gel method and the conventional melting process [23]. The sol-gel-synthesized BGs are produced at lower temperatures without the evaporation of volatile P_2O_5 with better chemical homogeneity and higher purity [24].

As mentioned above, both Sr and Li have played a critical role in the bone remodeling process and have been used individually as the doping elements in modified BGs. Until now, no studies have been reported on the synthesis and in vitro properties of the simultaneous addition of Sr and Li on SiO_2-CaO-P_2O_5 system. In this project, 58S bioglass

Mehrnaz Aminitabar is with the Scientific and technology park, Imam Khomeini International University, Qazvin, 34149-16818, Iran (corresponding author, phone: +98 9361369177, fax: +09833901186, e-mail: aminitabar.m@gmail.com).

Moghan Amirhosseinian is with the Scientific and technology park, Imam Khomeini International University, Qazvin, 34149-16818, Iran, Department of Materials Engineering, Imam Khomeini International University, Qazvin, 34149-16818, Iran and Harvard-MIT Division of Health Sciences and Technology, Massachusetts Institute of Technology, Cambridge 02139, MA, USA.

Morteza Elsa is with the Scientific and technology park, Imam Khomeini International University, Qazvin, 34149-16818, Iran.

incorporated with both Sr (with a concentration range of 0 to10 mol%) and Li (with a concentration range of 0, to 10 mol%) were synthesized through the sol-gel route. Inductively coupled plasma atomic emission spectroscopy (ICP-AES) was used for the analysis of Ca, Si, Sr, and Li to measure ionic concentration in the SBF solution, and system pH was monitored over time. In addition, the physicochemical characterization of the phases formed at the synthesized BG surface was accomplished using Fourier transform infrared spectroscopy (FTIR), X-ray diffraction (XRD), and scanning electron microscope (SEM) analyses. Furthermore, ALP activity measurement and methylthiazol tetrazolium (MTT) assay were performed for *in vitro* biological investigation. Afterwards, Live-Dead cell staining technique was performed. In order to assess cell viability qualitatively in presence of Li in BG and also Actin staining of cells was carried out for the visualization of the actin fibers and nuclei of MC3T3-E1 cells. Eventually, bactericidal efficiency of synthesized BGs was evaluated against MRSA bacteria.

II. Materials and Method

A. Materials

For synthesis of BGs, Tetraethyl orthosilicate (TEOS) and triethyl phosphate (TEP) were used as a liquid precursor for silica and phosphate, respectively. Also, calcium nitrate tetrahydrate $Ca(NO_3)_2.4H_2O$, strontium nitrate $Sr(NO_3)_2$ and lithium nitrate $LiNO_3$ were used as sources of CaO, SrO, and Li_2O in BG composition. Additionally, to study the *in vitro* bioactivity, the SBF solution was prepared according to the Kokubo procedure by using NaCl, KCl, $K_2HPO_4.3H_2O$, $MgCl_2.6H_2O$, $CaCl_2$, Na_2SO_4 reagents, tris (hydroxymethyl) aminomethane $(HOCH_2)_3CNH_2$, and HCl as described in the literature [25]. All the chemicals are purchased from Merck KGaA (Germany) and used directly without further purification. For proliferation and ALP activity investigation, MC3T3-E1, a mouse osteoblast-like cell line, was purchased from Sigma-Aldrich (Poole, UK). Cells maintained at 37 °C in a humidified, 5% CO_2, 95% air atmosphere under standard conditions and in α-MEM supplemented with 10% fetal bovine serum (FBS), (Sigma-Aldrich, UK), 1% antibiotic, 2 mM glutamine and 0.1% penicillin-streptomycin. The culture medium was changed every 2 days. The confluent cells were dissociated with trypsin and sub cultured to three passages which were used for tests. The medium was replaced every 2 days and confluent cells were subcultured through trypsinization.

B. BG Synthesis

The sol-gel route was used to synthesize SiO_2-CaO-P_2O_5-SrO-Li_2O BG. The compositions of the BG are listed in Table I. For the synthesis of the BGs a 1 M nitric acid solution was prepared and then TEOS (Merck) was added to the solution and the mixture stirred for 1h. This was followed by the addition of TEP (Merck) in a dropwise manner and the solution was kept stirring for another hour. Then, calcium nitrate tetrahydrate [$Ca(NO_3)_2$.4H2O, pure, Merck], and based on the composition, required amount of strontium nitrate [$Sr(NO_3)_2$, pure, Merck] and lithium nitrate [$LiNO_3$, Merck] were added slowly to the solution with 45 min interval between each addition for complete dissolution of the nitrates. The final mixture was stirred for 1 hour to obtain a homogenous and transparent sol. Afterwards, the synthesized sol was poured into a Pyrex container and aged for 3 days in 37 °C to produce the gels and subsequently the gels were heated for 3 days in 75 °C. Finally, the gels were milled in a planetary ball-mill before being stabilized for 3h at 700 °C as determined by TGA/DTA analysis to remove the residual nitrate and organic substances. The stabilized powders were cooled in the furnace at the rate of 5 °C/min and milled again to obtain powder with a particle size below 50 μm. For biological investigation, disc-shaped specimens (Ø10×3 mm) were prepared by pressing the powders in a die with a hydraulic press under 9 MPa pressure. In addition, prior to cell culture experiments, BG discs were sterilized under UV light for 2h on each side and preconditioned in 1 mL of culture medium. The culture medium was changed every day [26].

C. Characterization of BGs

The thermal behavior of dried gels was investigated by thermo gravimetric and differential thermal analyses (Shimadzu DSC-50 apparatus). For this purpose, 10 mg of dried gel of BG and BG-10/10 were heated up to 1100 °C in a platinum crucible under a N_2 atmosphere (50 mL/min) at a constant rate of 10 °C/min. For the analysis of changes in phase composition before and after soaking in SBF, XRD (INEL-Equinox-3000, France) was performed on BGs surfaces by applying a Cu Kα X-ray at 40 kV and 0.15406 nm wavelength in a 2θ range of 20°–50°.

TABLE I
Nominal Composition of BGs (in mol%)

Glass	Label	SiO_2	CaO	P_2O_5	SrO	Li_2O
58S	BG-0/0	60	36	4	0	0
58S -5 % Sr-5 % Li	BG-5/5	60	26	4	5	5
58S -5 % Sr-10 % Li	BG-5/10	60	21	4	5	10
58S -10 % Sr-5 % Li	BG-10/5	60	21	4	10	5
58S -10 % Sr-5 % Li	BG-10/10	60	16	4	10	10

An FTIR (Nicolet Avatar 660, Nicolet, USA) was employed in the wavenumber range of 400–4000 cm^{-1} to investigate the apatite phase formation on the surface of specimens. Moreover, the morphology of the formed apatite on the BGs surface was investigated over time by scanning electron microscopy (SEM, Philips XL30, Netherland) at an acceleration voltage of 10 kV after being coated by gold on the surfaces.

The disk-shaped BGs were soaked in SBF at 37 °C for 1, 3, 7, and 14 days. The ratio of the sample surface area to the SBF volume was approximately 0.1 $cm^2.mL^{-1}$. At the selected immersion time periods, based on chemical changes of the BGs [27], the concentrations of Ca, Si, P, Sr and Li ions in SBF solution were measured and evaluated by inductively coupled plasma atomic emission spectroscopy (ICP-OES;

Varian Vista Pro, Palo Alto, USA).

D. Biological Evaluation

1. MTT Assay

MTT assay, based on the reduction of tetrazolium salt to formazan crystals by living cells was carried out on three samples of each glass to evaluate viability and proliferation of cells seeded on the synthesized BGs in 24-well cell culture plates for 1, 3 and 7 days. First, 100 µL of a 5 $mg.mL^{-1}$ solution of MTT in phosphate buffered saline (PBS) was added to the culture media of live cells at the end of each mentioned time points. After 4 h incubation at 37 °C in a fully humidified atmosphere at 5% CO_2 in air, media was removed and the formazan was solubilized in dimethyl sulfoxide (DMSO, Sigma). The absorbance of the solutions was read on a microplate reader (EL 312e Biokinetics reader, Biotek Instruments) at 570 nm compared to three wells in the absence of glass samples were used as controls [28].

2. ALP Activity

The osteoblastic activity was investigated accordingly to the manufacturer's recommendations (BioCat, Heidelberg, Germany) by using the ALP kit (Sigma, St Louis, USA) as one of the osteoblastic differentiation markers [29]. For this purpose, MC3T3-E1 cells were counted and plated in 24-well plates at a density of 1×10^4 $cells.cm^{-2}$ and cultured on samples in a humidified atmosphere of 95% air and 5% carbon dioxide at 37 °C for 1, 3, and 7 days. Also, as negative controls, three wells in the absence of BGs were used. On day 1, 3, and 7 the supernatant fluid was removed gently and the cell layer was rinsed well with PBS, homogenized with 1 mL Tris buffer and sonicated for 4 min on ice. Aliquots of 20 µl were placed in equal volumes of 1ml of a p-nitrophenyl phosphate solution (16 mM, Sigma, St Louis, USA) and were incubated at 30 °C for up to 5 min. Cellular ALP activity was identified by the conversion of p-nitrophenyl phosphate to p-nitrophenol and absorption was measured at 410 nm as previously described [30].

3. Live-Dead Assay

To observe the simultaneous effect of Sr and Li in BGs composition, live/dead cell staining technique in presence of BG (as a control) and BG-5/5 (as a peak sample based on MTT) was applied as previously described to qualitatively identify the cell viability [26]. For this purpose, MC3T3-E1 cells were seeded at a density of 2.5 × 106 $cells.mL^{-1}$ in presence of BG-0/0 and BG-5/5 samples with the media exchanged at 48-hour intervals. After 1 day culture, cell culture media were removed and cell-seeded samples were washed twice with phosphate buffered saline (PBS) gently and incubated with 300 µL of 0.5 µM calcein-acetoxymethyl ester (calcein-AM, Sigma, USA) and 2 µM ethidium homodimer-1 (EthD-1, Sigma, USA) as a live/dead assay solution at 37 °C in a humidified atmosphere of 5% CO_2 for 15 min in dark and cells were washed again with PBS. Stained cells (live: green; dead: red) were observed under Zeiss Axio Observer Z1 inverted microscope and representative images were taken.

4. Actin Staining of Cells

To visualize the morphology of actin fibers and nuclei of MC3T3, after 1 and 7 days, cells were fixed with 4% paraformaldehyde (Sigma, St Louis, USA) solution for 30 min at room temperature. To stain the nuclei, cells were incubated in a 0.1% (v/v) DAPI solution in PBS for 10 min at 37 °C. After three times washing with DPBS, the fluorescence images of the cells' nuclei were acquired. For actin cytoskeleton staining, first, cells permeabilized by using 0.1% (v/v) Triton X-100 (Sigma, paraformaldehyde (Sigma,)/PBS solution for 30 min and followed by 3-times washing with PBS, then cells were blocked in 1% (v/v) BSA/PBS solution for 1h. Finally, a 1/40 dilution of Alexa Fluor-594 phalloidin (Invitrogen, USA) in 0.1% BSA was added to cells and incubated 45 min at room temperature.

5. Antibacterial Studies

Staphylococcus aureus (MRSA) is type of Staphylococcus aureus, which is a major cause of hospital-acquired infections and is resistant to some antibiotics [31]. MRSA were cultured in liquid lysogenybroth (LB) medium at 37 °C. Before experiments, it was diluted approximately to 0.5- 2×10^8 mL^{-1} [32]. To investigate the simultaneous effect of Sr and Li on antibacterial activities in BGs, 0.9 ml LB medium was added into three sterile 1.5 mL Eppendorf tubes containing 10 mg BG (as a control), BG-5/5, BG-5/10, BG-10/5 and BG-10/10 particles followed by stirring for 1 min. Then 0.1 ml bacterial suspension added into each Eppendorf tube and the solutions cultured at 37 °C for 1 h. After a serial dilution, 100 µl suspensions were plated onto LB-agar plates and incubated over- night at 37 °C in the dark.

E. Statistical Analyses

The quantified results were presented as mean±standard deviation (SD) of at least five experiments. The statistical significance between the mean values was calculated using GraphPad Prism software package, version 3.0 (GraphPad Prism, USA) and the $p<0.05$ was considered statistically significant. ($^*p < 0.05$, $^{**}p < 0.01$, $^{***}p < 0.001$ and $^{****}p < 0.0001$)

III. Results and Discussions

A. Thermal Analysis

The DTA and TGA curves of BG-0/0 and BG-10/10 are shown in Figs. 1 (a) and (b). As previously shown [33], the first endothermic peak appeared at approximately 150 °C is related to the loss of physically adsorbed water in the glass network. The second and third peaks were referred to condensation of silanol groups and elimination of nitrates which were occurred at 390–430 °C and 435–465 °C, respectively. Above 700 °C, because of completion of reactions and release of the volatiles, no significant change in the mass was observed. The onset crystallization exothermic peak for BG-0/0 and BG-10/10 were observed at around 1000 °C and 900 °C, respectively. Previously it was reported that the substitution of SrO and Li_2O for CaO in BG composition resulted in a decrease of crystallization temperature [34]. For

instance, Pacheco et al. showed that crystallization temperature decreased approximatly 50 °C by 10 wt% substitution of Li_2O for CaO in lithium-releasing silicate BG [18]. Moreover, Salman et al. claimed that the replacement of strontium oxide instead of calcium oxide in Li_2O–CaO–SiO_2 glass led to the same result.

DTA/TGA Results showed that the simultaneous presence of Sr and Li in BG-10/10 resulted in a100 °C decrease in crystallization temperature compared with BG-0/0 due to the mixed alkali/alkaline earth effect. Rolling et al. showed that in a SiO_2-Na_2O-CaO-SrO glass the mobility of the alkaline-earth ions are increased when they are partially replaced by the alkali ion and as a result a small reduction in the glass transition temperature was observed [35]. It appears that Li ion with a smaller ionic radius compared to Na ion have a more pronounced effect on the glass transition temperature of the glass. Based on the DTA results 700 °C was selected for stabilization of all glasses.

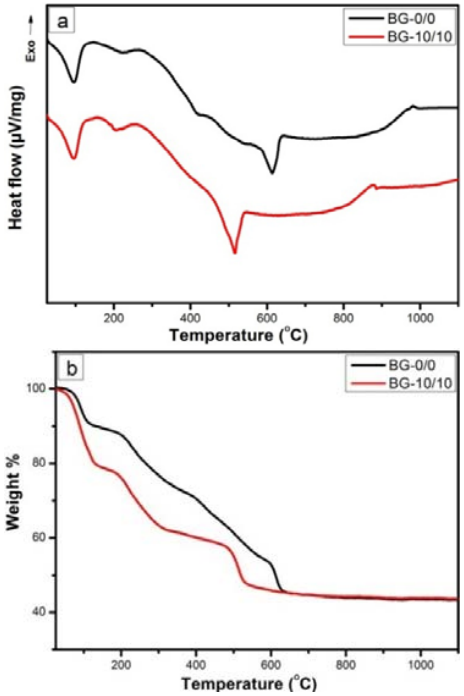

Fig. 1 (a) Differential thermal analysis (DTA) and (b) Thermogravimetric analysis (TGA) curves of as-prepared powder of BG-0 and BG-10/10 up to 1100 °C

B. Phase Analysis

Before immersion in SBF, XRD pattern of BG confirmed its amorphous structure and glassy nature with no characteristic peaks (Fig. 2 (a)). The XRD patterns for BG-0/0 and BG incorporated with both Sr and Li for different soaking periods up to 14 days in SBF were presented in Figs. 2 (a)-(f). After 1 day of immersion, structures of BG surfaces were remained amorphous and no distinctive peak was observed in the XRD patterns. According to the standard JCPDS cards (76-0694), the characteristic diffraction peaks at 25.8 and 31.8 (2θ) are assigned for (200) and (211) atomic planes in apatite lattice respectively. After 3 days of immersion, new peaks at 25.8 and 31.8 were appeared for BG, BG-5/5 (Figs. 2 (a) and (b)). While, only one peak at 31.8 (2θ) was observed for BG-5/10 attributed to the crystallization of (112) atomic planes in apatite lattice and there was no diffraction peak detected for BG-10/5 and BG-10/10. After 7 days of immersion, a slight increase in the peaks intensity of the (200) and (211) were observed for BG-0/0, BG-5/5 and BG-5/10 due to enhancement of apatite crystallization and for BG-10/5 and BG-10/10 a peak at 31.8 ascribed for (211) atomic planes was observed (Figs. 2 (c)-(e)). For all BGs, a gradual increase in peak intensity of (211) planes were observed from day 7 to day14.

It was found that a simultaneous increase in the Sr and Li content in BG composition from 5 to 10 mol%, reduced the ability of in vitro apatite formation on the surfaces of BGs by comparing the peak intensity of the (002) and (211) in BGs XRD patterns. Meanwhile, BG-5/5 had a similar trend to BG in comparison to the others. Furthermore, the maturity of the formed apatite layer on BG-0/0 and BG-5/5 surface after 14 days was approved by detection of new peaks at 32.18 and 32.86 assigned to the crystallization of (112) and (300) atomic planes in apatite lattice, respectively (Figs. 2 (a) and (b)) [36]. Hence, from the XRD results, the bioactivity of BG-5/5 was comparable to BG-0/0 and higher than other Li and Sr substituted glasses by considering the peak intensity of the (002) and (211) atomic planes in apatite lattice at 25.8, 31.8 (2θ°) and also, peaks attributed to (112) and (300) atomic planes.

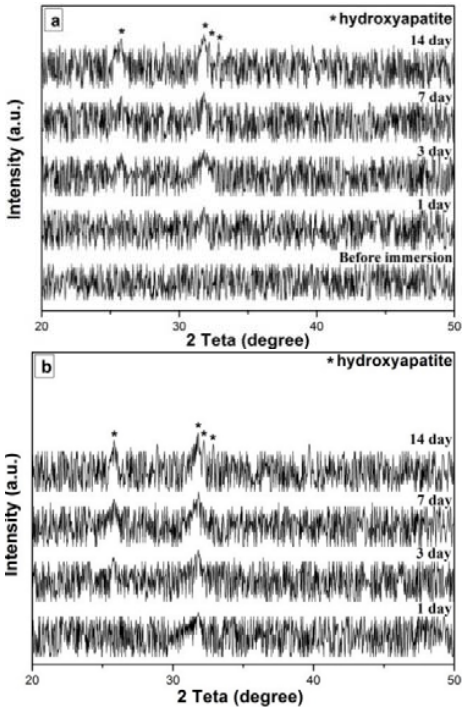

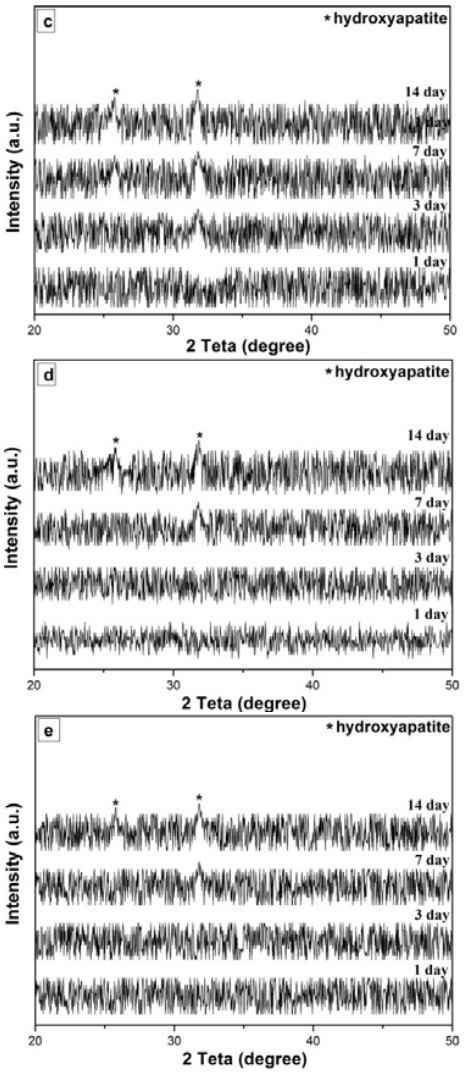

Fig. 2 The XRD patterns of BG-0/0 before and after immersion in SBF (a), BG-5/5 (b), BG-5/10 (c), BG-10/5 (d) and BG-10/10 (e) after 1, 3, 7 and 14 days soaking in SBF

C. Structural Groups

Figs. 3 (a)-(e) present the FTIR spectra of the synthesized BGs before and after immersing in SBF for time periods of 1, 3, 7 and 14 days. The main infrared bands appeared at 470, 790, 922, 1066 and 1250 cm^{-1} were related to the silicate network and were assigned to, respectively, the Si–O–Si bending vibration, the Si–O symmetric stretching of bridging oxygen atoms between tetrahedrons, Si–O stretching of non-bridging oxygen atoms, Si–O–Si symmetric stretching and the Si–O– Si asymmetric stretching [37].

The band located at 609 cm^{-1} is attributed to the asymmetric vibration of $PO4^{3-}$ [38]. The stretching mode of the OH group (hydroxyl) appeared at 3500 and 1651 cm^{-1}. By increasing the immersion time, new peaks appeared in the FTIR spectra of samples that confirms apatite formation on the surface of the BGs [39]. After 3 days of immersion in SBF, two additional peaks at around 1455 cm^{-1} and 870 cm^{-1} were observed in FTIR spectra for BG-0/0, BG-5/5 and BG-5/10 in comparison to the BG-10/5 and BG-10/10 that were attributed to C–O stretching in carbonate groups substituted for phosphate groups in apatite lattice. In addition, The P–O absorption bands were seen as two resolved peaks with increased intensity at 570 and 600 cm^{-1} which are typical of crystalline apatite [40].

The FTIR spectra were in good agreement with XRD patterns by indicating the crystalline nature of the new formed material on the BG-0/0, BG-5/5 and BG-5/10 surfaces with characteristic peaks of bone-like apatite (at $2\theta = 26°$ and $2\theta = 32°$) at the immersion time of 3 days and the intensities increased by increasing the immersion time. These mentioned peaks were appeared for BG-10/5 and BG-10/10 after 7 days. The intensities of peaks were increased over time from day 7 to 14 due to enhancement of apatite formation on the surface of BGs.

Based on the definition introduced by Farlay et al. [41], the maturity of HA is the progressive transformation of nonapatitic domains into poorly crystallized and followed by crystallization of HA. Fig. 3 (f) shows the FTIR spectra of BG-0/0, BG-5/5, BG-5/10, BG-10/5 and BG-10/10 in range of 1070 to 1140 cm^{-1} after immersion for 14 days. The ratio of the area under FTIR spectra of synthesized samples was measured and divided by the area under FTIR spectrum of BG-0/0 (as a control) in the mentioned range. This ratio was in order 0.98, 0.91, 0.52 and 0.39 for BG-5/5, BG-5/10, BG-10/5 and BG-10/10, respectively. From these results, it was found that Sr had a more pronounced inhibiting effect on bioactivity compared with Li. Meanwhile, BG-5/5 had similar HA maturity compared to BG-0/0 which was in good accordance with XRD results by detection of new peaks at 32.18° and 32.86° assigned to the crystallization of (112) and (300) atomic planes in HA lattice. Therefore, From the FTIR investigation, BG-0/0, BG-5/5 and BG-5/10 had nearly similar bioactivity while the lowest bioactivity was found in BG-10/10 by considering intensities of the observed peaks.

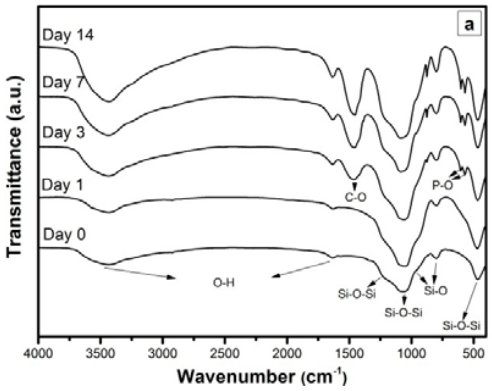

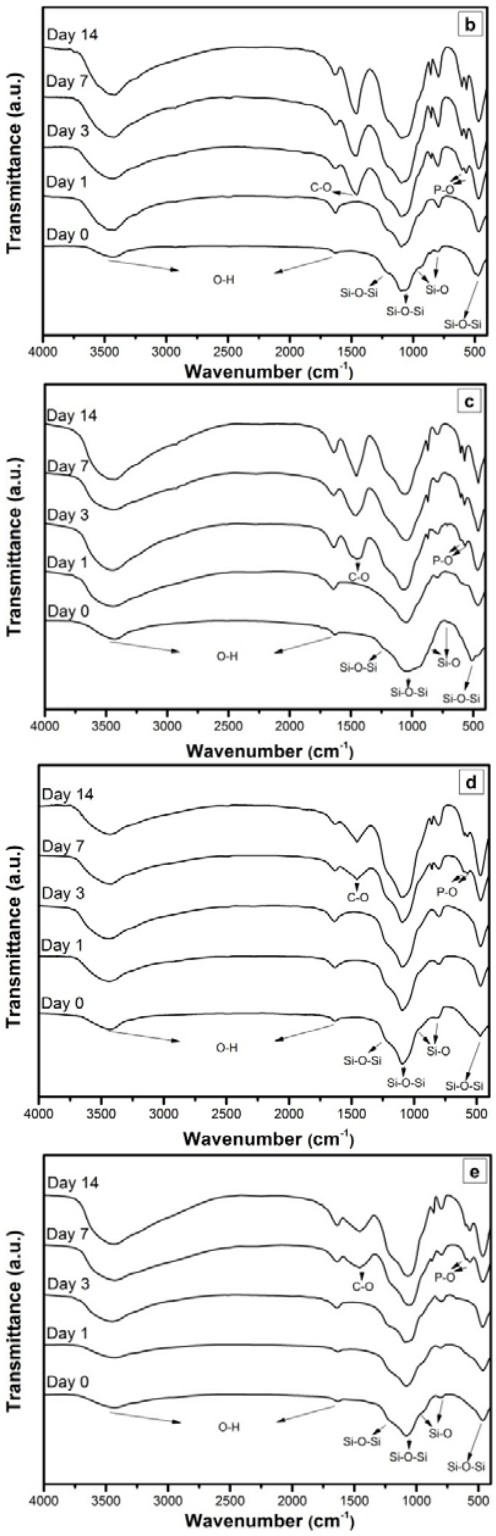

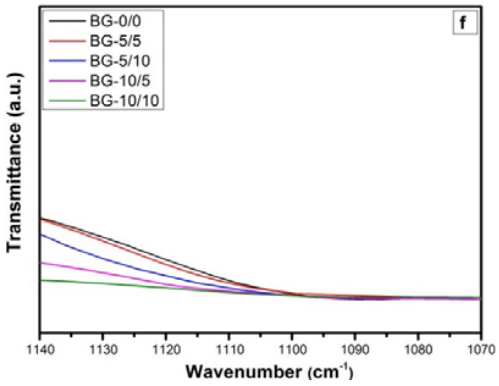

Fig. 3 The FTIR spectra of BG-0/0 (a), BG-5-5 (b), BG-5/10 (c), BG-10/5 (d) and BG-10/10 (e) before and after different soaking periods up to 14 days and FTIR spectra of all synthesized BGs in range of 1070 to 1140 cm^{-1} after 14 days soaking (f)

D. Ion Chemistry of SBF Solution

The changes in the ions concentration in the SBF solution with time is illustrated in Figs. 4 (a)-(e) and the SBF solution pH in Fig. 4 (f). As it is shown in Fig. 4 (a), the Ca concentrations of the BG-5/5, BG-5/10, BG-10/5 and BG-10/10 increased rapidly from ~100 mg/l in the SBF solution and the increase in the solution pH shows the ion exchange reaction with Ca^{2+} in the glass and H^{+} in the solution. The increase in the Ca concentration for the samples with 10 mol % Sr, i.e. BG-10/5 and BG-10/10, continued up to day 3 but all the other samples saw a sudden decrease in the Ca concentration on day 3. Based on the mechanisms suggested previously [3], this change in profile of Ca concentration is due to the dissolution of the Ca ions from the BGs followed by the precipitation of the Ca ions from SBF on the BGs surface and formation of HCA. This was approved by both XRD and FTIR results which showed no apatite peaks after first day immersion for BG-5/5 and BG-5/10. While for BG-10/5 and BG-10/10, no changes were observed in XRD and FTIR patterns up to day 7.

Fig. 4 (b) indicated a lower solubility of Si for the sample with high Li and low Sr content, i.e., BG-5/10 and in contrast the sample with low Li and high Sr, i.e., BG-10/5 had a higher Si release on day 1. This could be due to the effect of lower and higher ionic radius of Li and Sr in comparison to Ca, respectively, which results in a difference in the compactness of the glass structure and the rate of ion release. In other words, substitution of Ca^{2+} with Sr^{2+} in BG increased the BGs solubility by increasing the network disorder because of the difference in their ionic radius and the resulting decrease in the oxygen density [42]. On the other hand, the substitution of Ca^{2+} with Li^{+} had a reverse effect. This was in reasonable agreement with results by Demin et al. [43] who suggested that the substitution of low-dose strontium introduces more lattice distortions into the BG structure and consequently increases the solubility. Moreover, Hesaraki et al. [44] showed that the replacement of CaO by SrO in BG because of the higher ionic radius of Sr compared with Ca, led to a significant increase in glass solubility. By considering the Si

release in SBF solution as a solubility criterion, the dissolution rate was inversely proportional to oxygen density (OD) of the BGs. The possible mechanisms for the lower bioactivity were a lower supersaturation degree for nucleation of apatite and blocking of the active growth sites of calcium phosphate respectively by Li^{+} and Sr^{2+} in synthesized Li- Sr-substituted BGs. The oxygen densities of various substituted BG-58S are presented in Table II.

According to Figs. 4 (a) and (b), quick release of Ca and Si from BGs and subsequent apatite formation was the main factors in the rapid bonding of BGs to bone tissue and a higher bioactivity [45]. Figs. 4 (d) and (e) show that the rate of Sr and Li release is proportional to the concentration of those elements in the BG and both elements after an initial high rate of dissolution level off after day 7 of soaking in the SBF solution. Also, in general, a higher content of Sr in the BG composition slightly promotes the Li release into the SBF and conversely Li slightly demotes the rate of Sr release.

Ion exchange between Ca^{2+}, Sr^{2+}, Li^{+} from the BG and H^{+} from the SBF led to an increase in the pH value of the SBF in the early stages of the soaking of the sample but levels off after day 7 as the Ca concentration is precipitated in the form of HCA and its concentration in the solution reaches back to its initial value and at the same time the level of Sr and Li is stabilized in the SBF. Results show that Li had a slightly more pronounced effect in increasing the pH value of the solution probably because Li is a stronger base compared to Ca or Sr [38].

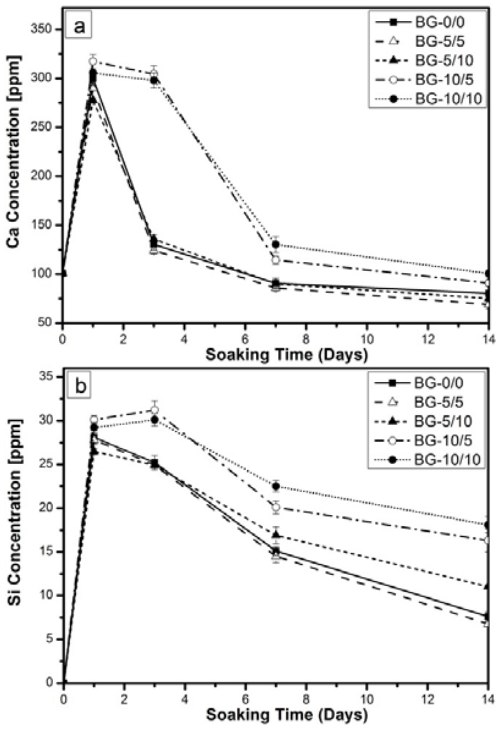

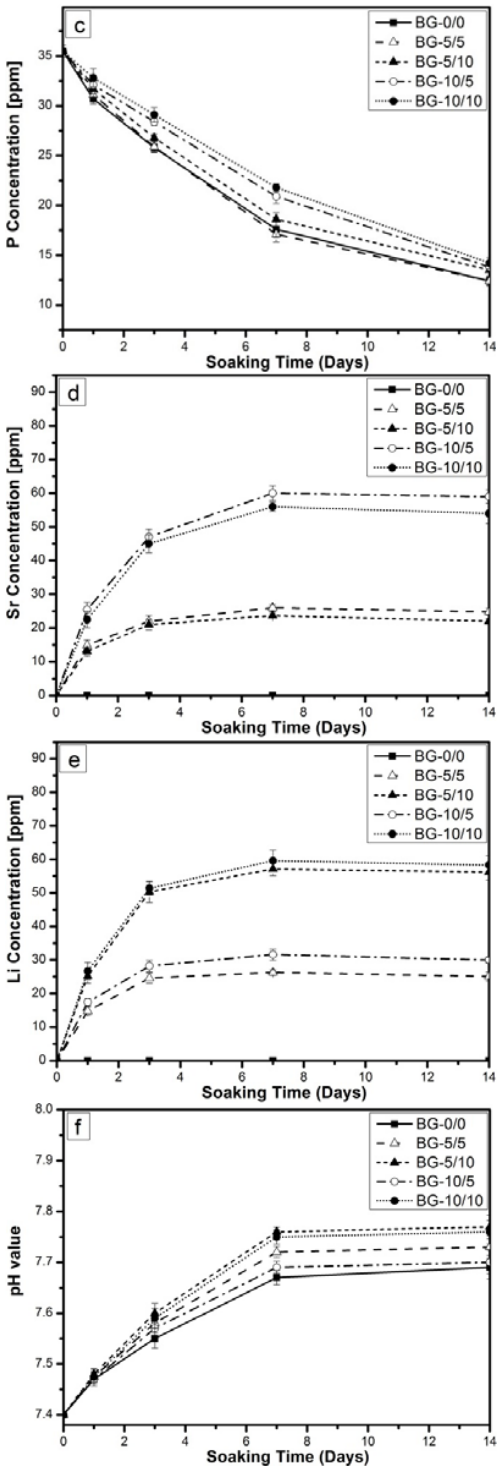

Fig. 4 Variation of elemental concentration and pH in the SBF with soaking time for calcium (a), silicon (b), phosphorous (c), strontium (d), lithium (e) and pH (f)

E. Surface Microstructures

The SEM micrograph of the synthesized BG-0/0 before soaking in the SBF in Fig. 5 (a) shows the surface of the glass with some large flaky particles. Figs. 5 (b)-(f) show the SEM

micrographs of all the samples after soaking in SBF for 14 days. At day 14, BG surfaces were covered with different shapes of apatite layer. On the surface of BG-0/0, a cauliflower-like apatite structures were observed, in contrast to the flake-like crystals with different abundance on other BGs surfaces. On the other hand, the layer on the BG-5/5 displayed a rod-like morphology (typically less than 100 nm in width). The formation of unexpected rod-like HA was previously reported by Taherkhani et al. [46] in presence of Sr in bioglass $60\%SiO_2–36\%(CaO/SrO)–4\%P_2O_5$,although the main reason for formation of such structure remains unknown [47].

From the SEM observation, BG-0/0, BG-5/5 and BG-5/10 had nearly similar HA formation ability while, the lowest HA formation capability was attributed to BG-10/10 by considering density of covered surface areas and it was in good agreement with FTIR and XRD results.

TABLE II
THE OXYGEN DENSITY OF SUBSTITUTED 58S BGS

BG	BG-0/0	BG-5/5	BG-5/10	BG-10/5	BG-10/10
Oxygen density	0.7560±0.001	0.7572±0.008	0.7584±0.001	0.7408±0.007	0.7485±0.002

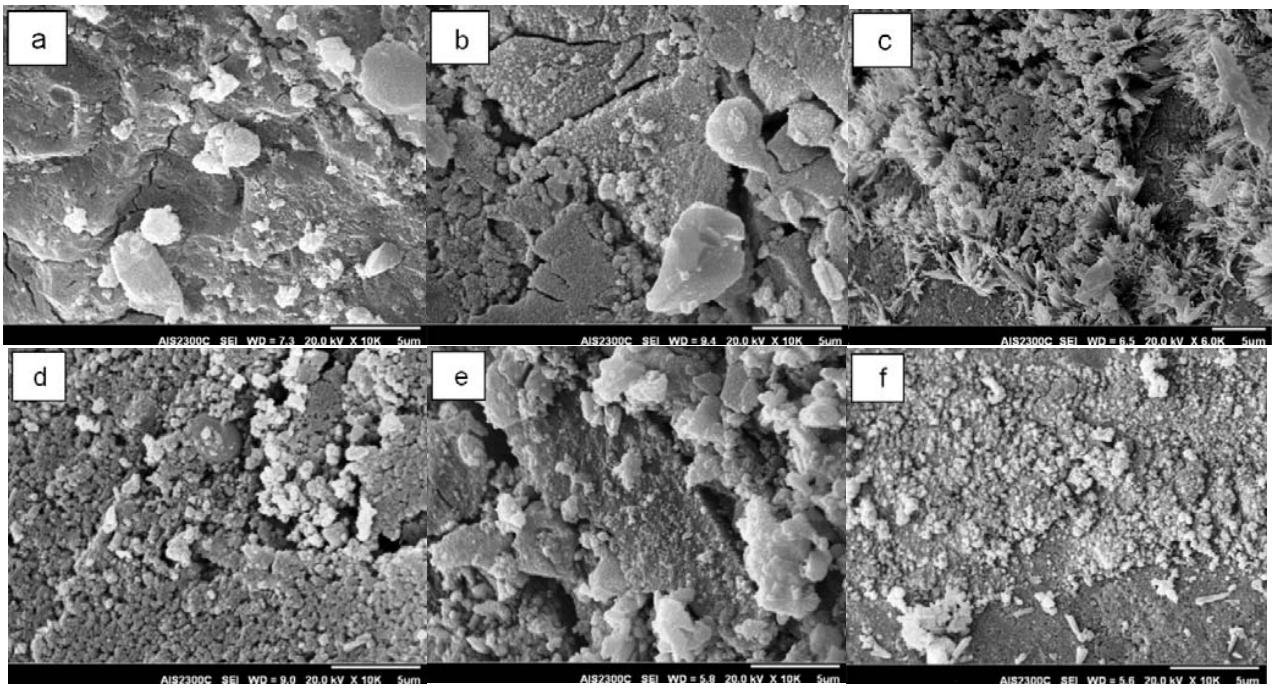

Fig. 5 SEM morphology of the surface of BG-0/0 disc before and after soaking in the SBF for 14 days (a) and morphology of the HA formed on disc samples after soaking in the SBF for 14 days respectively; BG-5/5 (b), BG-5/10 (c), BG-10/5 (d) and BG-10/10 (e)

F. In vitro Biological Evaluation

1. Cell Proliferation and Activity

The proliferation of the osteoblast-like cell line, MC3T3-E1, cultured on various specimens for different times is shown in Fig. 6. After 1 day in culture, there were no significant differences in the MTT activity of cells incubated with synthesized BGs with different amount of Sr and Li dissolution ions compared to control. After 3 days in culture, MTT activity was significantly higher in cells in presence of dissolution ions from BG-0/0, BG-5/5 and BG-5/10 compared to control. Meanwhile, cells in presence of BG-5/5 and BG-5/10 exhibited same proliferation with no statistically significant difference ($p>0.05$). Additionally, these values were increased over time and achieved their maximum after 7 days for BG-5/5 and BG-5/10. Based on the results of MTT assay, the simultaneous presence of Sr and Li enhanced the proliferation of MC3T3-E1 cells. The results of MTT assay was in good agreement with other works [48] because the growth and activity of the rat osteoblastic cells increased significantly by culturing them in contact with a BG containing little amount of SrO (5 mol%) or Li_2O (5 mol% or 10 mol%).

Zhang et al. [49] showed that 5 mol% Sr significantly increased the proliferation of bone marrow stromal cells (BMSCs) in a concentration dependent manner. Zhang et al. [50] observed an enhancement in proliferation of MC3T3-E1 cells treated with strontium substituted mesoporous bioglass (about 7 mol% Sr as a moderate level of Sr). Additionally, Liu et al. [51] and Hesaraki et al. [44] claimed that the presence of 5 mol% Sr in BG led to the best osteogenic promotion of MC3T3-E1 and rat calvaria-derived osteoblastic cells,

respectively. The cell proliferation was deceased by increasing the amount of Sr to more than 5 mol% in BG composition. Qiu et al. [52] described that the high concentration of Sr ions in the cell culture medium produces a cytotoxic effect on viability of osteoblastic cells., there are a few studies on the effect of Li in the BG composition on the cell proliferation [34] that shows Li^+ enhances the cell proliferation.

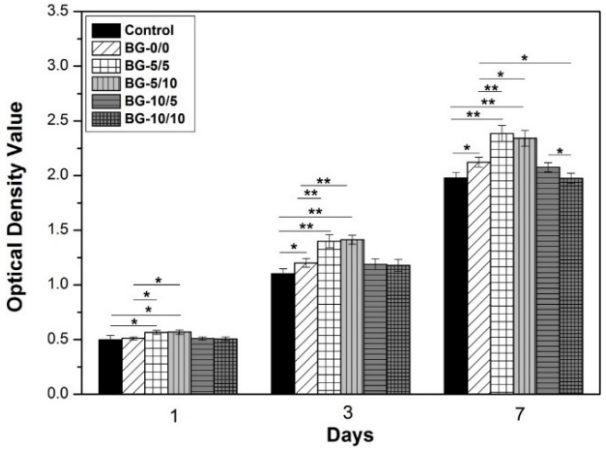

Fig. 6 The proliferation of the osteoblast-like cell line, MC3T3-E1, cultured on BG-0/0, BG-5 and BG-10 for 1, 3 and 7 days. (*p < 0.05, **p < 0.01 and ***p < 0.001)

Fig. 7 shows the normalized ALP activity of the osteoblast-like cell line, MC3T3-E1, cultured on the BGs for different periods of times. Results shows that the ALP activity of cells was increased from day 1 to 7 and it reached a maximum in day 7 to approximately 4-fold of its value in day 1. Additionally, for each culturing time, statistically significant differences were observed on BG-5/5, BG-5/10, BG-10/5 and BG-10/10 with respect to the control ($^*P< 0.05$). Meanwhile, the peak ALP activity was observed for the BG-5/5 and BG-5/10 with no significant statistically difference between the two (p> 0.05). Decreasing the ALP activity by increasing the Sr content from 5 to 10 (in mol%) was in agreement with the previous studies [53]. For instance, Hesaraki et al. [44]. claimed that the presence of 10 mol% Sr decreased the ALP activities of cells in contact with BGs in comparison to the sample with 5 mol% Sr. In addition, Wang et al. [54] also showed that low amount of Sr in BG enhanced the ALP activity of MSCs. Our results of the role of Li on the ALP activity conform to the other studies that investigated the role of Li on different BGs [55].

2. Live-Dead Assay and Actin Staining of Cells

The Live-Dead assay (Figs. 8 (a) and (b)) provided a direct observation of the proportion of living and dead cells**.** As it seen in Figs. 8 (a) and (b), after 1 day of culture, there were fewer dead cells treated by BG-5/5 in comparison with control (BG-0/0). Figs. 8 (c) and (d) display F-actin-labeled cytoskeleton of MC3T3-E on control and BG-5/5. It was observed that the cells adhered to both control (BG-0/0) and BG-5/5 exhibited abundant F-actin stress fibers. Moreover, the arrangement of F-actin fibers was randomly oriented and mainly in spindle-like elongated shape. The mean number of DAPI-labeled nuclei for BG-5/5 was more than the control which was probably due to the simultaneous presence of Sr and Li in the solution in composition with BG-5/5.

The staining results demonstrated that the BG-5/5 sample exhibited increased confluency with relatively fewer dead cells compared to the control sample on staining, suggesting a higher cell viability, which was in a close agreement with MTT results (Fig. 6). Meanwhile, Dapi/actin staining observation was in reasonable agreement with live/dead assay.

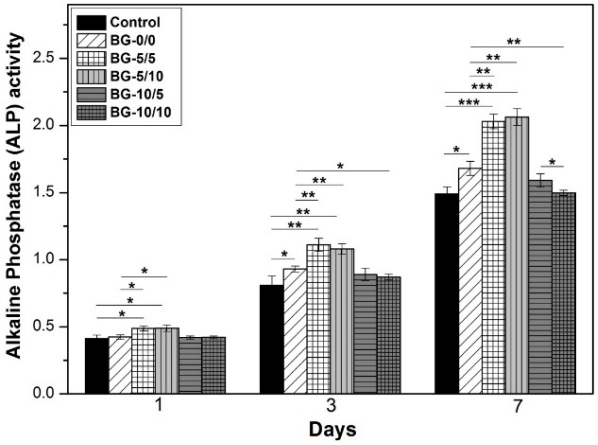

Fig. 7 The ALP activity of the osteoblast-like cell line, MC3T3-E1, cultured on BG samples for 1, 3 and 7 days. All data are presented as the mean values together with the standard deviation (*p < 0.05, **p < 0.01 and ***p < 0.001)

3. Antibacterial Studies

A bacterial infection can potentially lead to surgical failure [56]. The antibacterial effect of BGs was previously mentioned. This property is possibly attributed to the release of ions such as calcium and phosphate that have a toxic effect on the bacteria [57] and release of alkali ions which increases the pH value [32]. While, the exact mechanism responsible for the antimicrobial effect of BGs is not completely elucidated [57].

As seen in Fig. 9, the simultaneous presence of Sr and Li in 58S BGs led to a significant antibacterial effect against MRSA bacteria. Clearly, the samples with 5 mol% Li_2O (BG-5/5 and BG-10/5), with fixed concentration of 10 mg/ml in bacterial suspension, demonstrated the maximum bactericidal percentage to MRSA bacteria with no statistically significant difference (*P>0.05). Also, antibacterial activity decreased by increasing the Li in BG content (BG-5/10 and BG-10/10). Although the exact mechanism for the antibacterial effect of BGs remains unknown [57], some possible reasons are the presence of ions like calcium [57], phosphate [57], lithium [58] and strontium [59] and also, increase in the pH value due to release of alkali ions were proposed [60].

These results suggest that the simultaneous presence of Sr and Li in BG composition was more efficient in bactericidal activity than Sr and Li free 58S BG (BG-0/0).The highest

antibacterial activity was found for BG-5/5 and BG-10/5 (****$p < 0.0001$) with no statistically significant difference between them ($p > 0.05$) among the synthesized BGs.

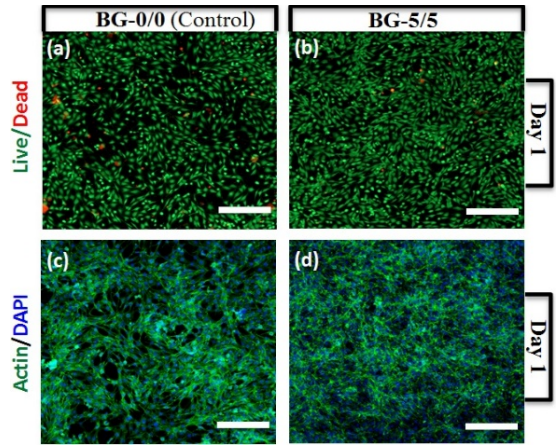

Fig. 8 Two dimensional (2D) MC-3T3 cells cultured in presence of BG-0/0 as a control and BG-5/5. Representative live/dead (a), (b) and Dapi/actin (c, d) fluorescence images of MC-3T3 cells cultured on BG-0/0 and BG-5/5 after 1 day of culture respectively. In live/dead staining, green fluorescent cells are alive and red fluorescent cells indicate dead cells. Additionally, in Dapi/actin staining, cell filaments are stained by Actin (green) and nuclei stained by DAPI (blue). Scale bar represents 100 μm in all images

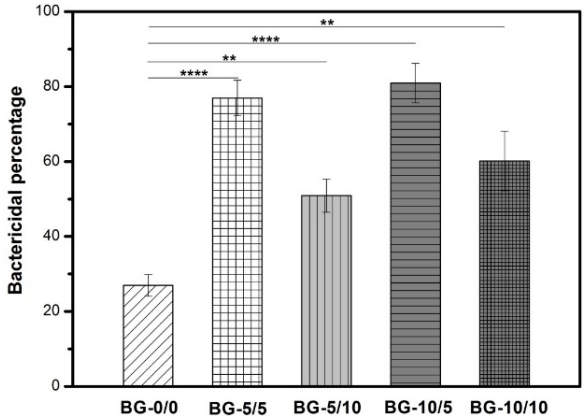

Fig. 9 The bactericidal percentages of 10 mg/ml of BG-0/0 (Control), BG-5/5, BG-5/10, BG-10/5 and BG-10/10

IV. Conclusion

In summary, 58S BGs incorporated with both Sr and Li (with a concentration range of 0, to 10 mol%) were synthesized through the sol-gel route and the synergetic effect of Sr and Li on BGs was investigated.

DTA/TGA results revealed that the simultaneous presence of Sr and Li in BG-10/10 resulted in a 100 °C decrease in crystallization temperature compared with the BG-0/0 due to the mixed alkali/alkaline earth effect. The appearance of C–O stretching and P–O absorption bands in FTIR spectra and the detection characteristic peaks of crystalline apatite phase as well as the surface morphology observation confirmed the formation of a crystalline HA on the surface of Sr and Li-doped 58S BGs after soaking in SBF solution. Meanwhile, by considering the ratio of the area under FTIR spectra of synthesized samples in range of 1070 to 1140 cm^{-1} after immersion for 14 days, it was concluded that BG-0/0 and BG-5/5 had nearly similar bioactivity which was in good agreement with XRD results. Moreover, in vitro experiments with MC3T3-E1 cells indicated that the simultaneous substitution of Sr and Li in the 58S-BG composition not only caused any cytotoxic effect but also had a stimulating effect on both differentiation and proliferation of MC3T3-E1s.

Eventually, based on biological and cell staining results, 58S BG incorporated with 5 mol% SrO and 5 mol% Li_2O (BG/5-5), significantly increased cell proliferation and ALP activity. On the other hand, BG-5/5 exhibited the highest bactericidal efficiency against MRSA bacteria. Therefore, BG-5/5 is suggested as a novel candidate with multi-function properties for bone tissue engineering. Further investigations are needed to clarify the exact mechanisms for simultaneous effect of Sr and Li dopants on increasing of antibacterial activity in synthesized novel biomaterial in future clinical applications.

References

[1] L. L. Hench, The story of Bioglass®, J. Mater. Sci. Mater. Med. 17 (2006) 967–978. doi:10.1007/s10856-006-0432-z.
[2] Y. Ebisawa, T. Kokubo, K. Ohura, T. Yamamuro, Bioactivity of CaO.SiO2-based glasses:in vitro evaluation, J. Mater. Sci. Mater. Med. 1 (1990) 239–244. doi:10.1007/BF00701083.
[3] L. L. Hench, J. Wilson, An Introduction to Bioceramics, World Scientific, 1993. doi:10.1142/2028.
[4] A. Moghanian, S. Firoozi, M. Tahriri, Characterization, in vitro bioactivity and biological studies of sol-gel synthesized SrO substituted 58S bioactive glass, Ceram. Int. 43 (2017) 14880–14890. doi: 10.1016/J.CERAMINT.2017.08.004.
[5] A. Moghanian, A. Sedghi, A. Ghorbanoghli, E. Salari, The effect of magnesium content on in vitro bioactivity, biological behavior and antibacterial activity of sol–gel derived 58S bioactive glass, Ceram. Int. (2018). doi: 10.1016/J.CERAMINT.2018.02.159.
[6] L. Courthéoux, J. Lao, J.-M. Nedelec, E. Jallot, Controlled Bioactivity in Zinc-Doped Sol−Gel-Derived Binary Bioactive Glasses, (2008).
[7] C. Wu, Y. Zhou, M. Xu, P. Han, L. Chen, J. Chang, Y. Xiao, Copper-containing mesoporous bioactive glass scaffolds with multifunctional properties of angiogenesis capacity, osteostimulation and antibacterial activity, Biomaterials. 34 (2013) 422–433. doi: 10.1016/j.biomaterials.2012.09.066.
[8] B. Akkopru, C. Durucan, Preparation and microstructure of sol-gel derived silver-doped silica, J. Sol-Gel Sci. Technol. 43 (2007) 227–236. doi:10.1007/s10971-007-1561-7.
[9] A. Moghanian, S. Firoozi, M. Tahriri, Synthesis and in vitro studies of sol-gel derived lithium substituted 58S bioactive glass, Ceram. Int. 43 (2017) 12835–12843. doi: 10.1016/j.ceramint.2017.06.174.
[10] I. D. Xynos, A. J. Edgar, L. D. K. Buttery, L. L. Hench, J. M. Polak, Ionic Products of Bioactive Glass Dissolution Increase Proliferation of Human Osteoblasts and Induce Insulin-like Growth Factor II mRNA Expression and Protein Synthesis, Biochem. Biophys. Res. Commun. 276 (2000) 461–465. doi:10.1006/bbrc.2000.3503.
[11] J. R. Jones, L. M. Ehrenfried, P. Saravanapavan, L. L. Hench, Controlling ion release from bioactive glass foam scaffolds with antibacterial properties, J. Mater. Sci. Mater. Med. 17 (2006) 989–996. doi: 10.1007/s10856-006-0434-x.
[12] A. Hoppe, N. S. Güldal, A. R. Boccaccini, A review of the biological response to ionic dissolution products from bioactive glasses and glass-ceramics, Biomaterials. 32 (2011) 2757–2774. doi: 10.1016/j.biomaterials.2011.01.004.
[13] S. Murphy, A. W. Wren, M. R. Towler, D. Boyd, The effect of ionic dissolution products of Ca–Sr–Na–Zn–Si bioactive glass on in vitro

cytocompatibility, J. Mater. Sci. Mater. Med. 21 (2010) 2827–2834. doi: 10.1007/s10856-010-4139-9.
[14] A. Moghanian, S. Firoozi, M. Tahriri, A. Sedghi, A comparative study on the in vitro formation of hydroxyapatite, cytotoxicity and antibacterial activity of 58S bioactive glass substituted by Li and Sr, Mater. Sci. Eng. C. 91 (2018) 349–360. doi: 10.1016/J.MSEC.2018.05.058.
[15] P. Habibovic, J. Barralet, Bioinorganics and biomaterials: bone repair, Acta Biomater. (2011).
[16] M. Arioka, F. Takahashi-Yanaga, M. Sasaki, T. Yoshihara, S. Morimoto, M. Hirata, Y. Mori, T. Sasaguri, Acceleration of bone regeneration by local application of lithium: Wnt signal-mediated osteoblastogenesis and Wnt signal-independent suppression of osteoclastogenesis, Biochem. Pharmacol. 90 (2014) 397–405. doi: 10.1016/j.bcp.2014.06.011.
[17] P. Han, C. Wu, J. Chang, Y. Xiao, The cementogenic differentiation of periodontal ligament cells via the activation of Wnt/β-catenin signalling pathway by Li+ ions released from bioactive scaffolds, Biomaterials. (2012).
[18] A. Zamani, G. Omrani, M. Nasab, Lithium's effect on bone mineral density, Bone. (2009).
[19] M. Khorami, S. Hesaraki, A. Behnamghader, H. Nazarian, S. Shahrabi, In vitro bioactivity and biocompatibility of lithium substituted 45S5 bioglass, Mater. Sci. Eng. C. 31 (2011) 1584–1592. doi: 10.1016/j.msec.2011.07.011.
[20] Z. Zhu, J. Yin, J. Guan, B. Hu, X. Niu, D. Jin, Y. Wang, C. Zhang, Lithium stimulates human bone marrow derived mesenchymal stem cell proliferation through GSK-3β-dependent β-catenin/Wnt pathway activation, FEBS J. 281 (2014) 5371–5389. doi:10.1111/febs.13081.
[21] A. Balamurugan, G. Sockalingum, J. Michel, J. Fauré, V. Banchet, L. Wortham, S. Bouthors, D. Laurent-Maquin, G. Balossier, Synthesis and characterisation of sol gel derived bioactive glass for biomedical applications, 2006. doi: 10.1016/j.matlet.2006.03.102.
[22] M. Vallet-Regí, C. V. Ragel, A. J. Salinas, Glasses with Medical Applications, Eur. J. Inorg. Chem. 2003 (2003) 1029–1042. doi:10.1002/ejic.200390134.
[23] P. Sepulveda, J. R. Jones, L. L. Hench, In vitro dissolution of melt-derived 45S5 and sol-gel derived 58S bioactive glasses, J. Biomed. Mater. Res. 61 (2002) 301–311. doi:10.1002/jbm.10207.
[24] D. Arcos, D. C. Greenspan, M. Vallet-Regí, A new quantitative method to evaluate the *in vitro* bioactivity of melt and sol-gel-derived silicate glasses, J. Biomed. Mater. Res. Part A. 65A (2003) 344–351. doi:10.1002/jbm.a.10503.
[25] T. Kokubo, H. Kushitani, S. Sakka, T. Kitsugi, T. Yamamuro, Solutions able to reproducein vivo surface-structure changes in bioactive glass-ceramic A-W3, J. Biomed. Mater. Res. 24 (1990) 721–734. doi:10.1002/jbm.820240607.
[26] E. Gentleman, M. M. Stevens, R. G. Hill, D. S. Brauer, Surface properties and ion release from fluoride-containing bioactive glasses promote osteoblast differentiation and mineralization in vitro, Acta Biomater. 9 (2013) 5771–5779. doi: 10.1016/j.actbio.2012.10.043.
[27] M. D. O 'donnell, R.G. Hill, Influence of strontium and the importance of glass chemistry and structure when designing bioactive glasses for bone regeneration, (2010). doi: 10.1016/j.actbio.2010.01.006.
[28] E. Gentleman, Y. C. Fredholm, G. Jell, N. Lotfibakhshaiesh, M. D. O'Donnell, R. G. Hill, M. M. Stevens, The effects of strontium-substituted bioactive glasses on osteoblasts and osteoclasts in vitro, Biomaterials. 31 (2010) 3949–3956. doi: 10.1016/j.biomaterials.2010.01.121.
[29] Y. Gotoh, K. Hiraiwa, M. Nagayama, In vitro mineralization of osteoblastic cells derived from human bone., Bone Miner. 8 (1990) 239–50. http://www.ncbi.nlm.nih.gov/pubmed/2157512.
[30] C. E. Yellowley, Z. Li, Z. Zhou, C. R. Jacobs, H. J. Donahue, Functional Gap Junctions Between Osteocytic and Osteoblastic Cells, J. Bone Miner. Res. 15 (2010) 209–217. doi:10.1359/jbmr.2000.15.2.209.
[31] M. C. Enright, D. A. Robinson, G. Randle, E. J. Feil, H. Grundmann, B. G. Spratt, The evolutionary history of methicillin-resistant *Staphylococcus aureus* (MRSA)., Proc. Natl. Acad. Sci. U. S. A. 99 (2002) 7687–92. doi: 10.1073/pnas.122108599.
[32] S. Hu, J. Chang, M. Liu, C. Ning, Study on antibacterial effect of 45S5 Bioglass®, J. Mater. Sci. Mater. Med. 20 (2009) 281–286. doi: 10.1007/s10856-008-3564-5.
[33] G. S. Lázaro, S. C. Santos, C. X. Resende, E.A. dos Santos, Individual and combined effects of the elements Zn, Mg and Sr on the surface reactivity of a SiO2·CaO·Na2O·P2O5 bioglass system, J. Non. Cryst. Solids. 386 (2014) 19–28. doi: 10.1016/j.jnoncrysol.2013.11.038.
[34] F. Baino, G. Novajra, V. Miguez-Pacheco, C. Vitale-Brovarone, Bioactive glasses: Special applications outside the skeletal system, J. Non. Cryst. Solids. 432 (2016) 15–30. doi: 10.1016/J.JNONCRYSOL.2015.02.015.
[35] B. Roling, M. Ingram, Mixed alkaline-earth effects in ion conducting glasses, J. Non. Cryst. Solids. 265 (2000) 113–119. doi: 10.1016/S0022-3093(99)00899-6.
[36] S. Shahrabi, S. Hesaraki, S. Moemeni, M. Khorami, Structural discrepancies and in vitro nanoapatite formation ability of sol–gel derived glasses doped with different bone stimulator ions, Ceram. Int. 37 (2011) 2737–2746. doi: 10.1016/j.ceramint.2011.04.025.
[37] X. Wu, G. Meng, S. Wang, F. Wu, W. Huang, Z. Gu, Zn and Sr incorporated 64S bioglasses: Material characterization, in-vitro bioactivity and mesenchymal stem cell responses, Mater. Sci. Eng. C. 52 (2015) 242–250. doi: 10.1016/j.msec.2015.03.057.
[38] M. Mozafari, F. Moztarzadeh, M. Tahriri, Investigation of the physico-chemical reactivity of a mesoporous bioactive SiO2–CaO–P2O5 glass in simulated body fluid, J. Non. Cryst. Solids. 356 (2010) 1470–1478. doi: 10.1016/j.jnoncrysol.2010.04.040.
[39] V. K. Vyas, A. S. Kumar, S. Prasad, S. P. Singh, R. Pyare, Bioactivity and mechanical behaviour of cobalt oxide-doped bioactive glass, Bull. Mater. Sci. 38 (2015) 957–964. doi:10.1007/s12034-015-0936-6.
[40] K. Zhang, H. Yan, D. C. Bell, A. Stein, L. F. Francis, Effects of materials parameters on mineralization and degradation of sol-gel bioactive glasses with 3D-ordered macroporous structures, J. Biomed. Mater. Res. 66A (2003) 860–869. doi: 10.1002/jbm.a.10093.
[41] D. Farlay, G. Panczer, C. Rey, P. D. Delmas, G. Boivin, Mineral maturity and crystallinity index are distinct characteristics of bone mineral, J. Bone Miner. Metab. 28 (2010) 433–445. doi: 10.1007/s00774-009-0146-7.
[42] J. Zeglinski, M. Nolan, M. Bredol, A. Schatte, S. A. M. Tofail, J. Kost, S. Bauer, M. Krause, W. W. Lu, Unravelling the specific site preference in doping of calcium hydroxyapatite with strontium from ab initio investigations and Rietveld analyses, Phys. Chem. Chem. Phys. 14 (2012) 3435. doi: 10.1039/c2cp23163h.
[43] C. Demin, F. Yuanfei, G. Guozhen, Preparation and solubility of the solid solution of strontium substituted hydroxyapatite, Chinese J. (2001). http://en.cnki.com.cn/Article_en/CJFDTOTAL-ZSWY200103015.htm (accessed May 27, 2017).
[44] S. Hesaraki, M. Gholami, S. Vazehrad, S. Shahrabi, The effect of Sr concentration on bioactivity and biocompatibility of sol–gel derived glasses based on CaO–SrO–SiO2–P2O5 quaternary system, Mater. Sci. Eng. C. 30 (2010) 383–390. doi: 10.1016/j.msec.2009.12.001.
[45] J. R. Jones, New trends in bioactive scaffolds: The importance of nanostructure, J. Eur. Ceram. Soc. 29 (2009) 1275–1281. doi: 10.1016/j.jeurceramsoc.2008.08.003.
[46] S. Taherkhani, F. Moztarzadeh, Influence of strontium on the structure and biological properties of sol–gel-derived mesoporous bioactive glass (MBG) powder, J. Sol-Gel Sci. Technol. 78 (2016) 539–549. doi:10.1007/s10971-016-3995-2.
[47] P. G. Koutsoukos, G. H. Nancollas, Influence of strontium ion on the crystallization of hydroxyapatite from aqueous solution, J. Phys. Chem. 85 (1981) 2403–2408. doi:10.1021/j150616a022.
[48] H. Attar, K. G. Prashanth, A. K. Chaubey, M. Calin, L. C. Zhang, S. Scudino, J. Eckert, Comparison of wear properties of commercially pure titanium prepared by selective laser melting and casting processes, Mater. Lett. 142 (2015) 38–41. doi: 10.1016/J.MATLET.2014.11.156.
[49] Y. Zhang, L. Wei, J. Chang, R. J. Miron, B. Shi, S. Yi, C. Wu, G. Sayegh, V. Guarneri, K. Desrouleaux, J. Cui, A. Adamus, R. F. Gagel, G. N. Hortobagyi, Strontium-incorporated mesoporous bioactive glass scaffolds stimulating in vitro proliferation and differentiation of bone marrow stromal cells and in vivo regeneration of osteoporotic bone defects, J. Mater. Chem. B. 1 (2013) 5711. doi:10.1039/c3tb21047b.
[50] J. Zhang, S. Zhao, Y. Zhu, Y. Huang, M. Zhu, C. Tao, C. Zhang, Three-dimensional printing of strontium-containing mesoporous bioactive glass scaffolds for bone regeneration, Acta Biomater. 10 (2014) 2269–2281. doi: 10.1016/j.actbio.2014.01.001.
[51] J. Liu, S.C.F. Rawlinson, R.G. Hill, F. Fortune, Strontium-substituted bioactive glasses in vitro osteogenic and antibacterial effects, Dent. Mater. 32 (2016) 412–422. doi: 10.1016/j.dental.2015.12.013.
[52] K. Qiu, X. J. Zhao, C. X. Wan, C. S. Zhao, Y. W. Chen, Effect of strontium ions on the growth of ROS17/2.8 cells on porous calcium polyphosphate scaffolds, Biomaterials. 27 (2006) 1277–1286. doi: 10.1016/j.biomaterials.2005.08.006.

[53] K. L. Wong, C. T. Wong, W. C. Liu, H. B. Pan, M. K. Fong, W. M. Lam, W. L. Cheung, W. M. Tang, K. Y. Chiu, K. D. K. Luk, W. W. Lu, Mechanical properties and in vitro response of strontium-containing hydroxyapatite/polyetheretherketone composites, Biomaterials. 30 (2009) 3810–3817. doi: 10.1016/j.biomaterials.2009.04.016.

[54] X. Wang, X. Li, A. Ito, Y. Sogo, Synthesis and characterization of hierarchically macroporous and mesoporous CaO–MO–SiO2–P2O5 (M=Mg, Zn, Sr) bioactive glass scaffolds, Acta Biomater. 7 (2011) 3638–3644. doi: 10.1016/j.actbio.2011.06.029.

[55] P. Han, C. Wu, J. Chang, Y. Xiao, The cementogenic differentiation of periodontal ligament cells via the activation of Wnt/?-catenin signalling pathway by Li+ ions released from bioactive scaffolds, Biomaterials. 33 (2012) 6370–6379. doi: 10.1016/j.biomaterials.2012.05.061.

[56] K. Yuan, Y. Chan, K. Kung, Comparison of osseointegration on various implant surfaces after bacterial contamination and cleaning: a rabbit study., Int. J. (2014). http://search.ebscohost.com/login.aspx?direct=true&profile=ehost&scope=site&authtype=crawler&jrnl=08822786&AN=93923200&h=nPWjzUDarXRc1r4xj2lbdZ%2BNH3XEQkCbkc9jMVRTGZWWhHu4Z6mPuVh2Z7DRzHyyWkZe0UhVliwN6Q1eYmILmQ%3D%3D&crl=f (accessed March 5, 2017).

[57] D. Khvostenko, T. J. Hilton, J. L. Ferracane, J. C. Mitchell, J. J. Kruzic, Bioactive glass fillers reduce bacterial penetration into marginal gaps for composite restorations, Dent. Mater. 32 (2016) 73–81. doi: 10.1016/j.dental.2015.10.007.

[58] J. Lieb, Lithium and antidepressants: Stimulating immune function and preventing and reversing infection, Med. Hypotheses. 69 (2007) 8–11. doi: 10.1016/j.mehy.2006.12.005.

[59] J. Liu, S. Rawlinson, R. Hill, F. Fortune, Strontium-substituted bioactive glasses in vitro osteogenic and antibacterial effects, Dent. Mater. (2016). http://www.sciencedirect.com/science/article/pii/S0109564115005163 (accessed March 2, 2017).

[60] I. Allan, H. Newman, M. Wilson, Antibacterial activity of particulate Bioglass® against supra- and subgingival bacteria, Biomaterials. 22 (2001) 1683–1687. doi:10.1016/S0142-9612(00)00330-6.